

# IMPLEMENTING COULOMBS FRICTION FOR THE CALCULATION OF DOWNHOLE CARDS IN DEVIATED WELLS

Victoria Pons-Ehimeakhe  
Weatherford

## ABSTRACT

Currently downhole cards can be computed from surface cards by solving the one dimensional damped wave equation with finite differences and an iteration on the damping factor or dual iteration on the damping factors. The one dimensional damped wave equation only takes into consideration friction of a viscous nature and ignores any type of mechanical friction. However, when dealing with a deviated or horizontal well, the mechanical friction in between the rods, couplings and tubing is no longer negligible. In this paper, the modified Everitt-Jennings code is further extended to incorporate mechanical friction and accommodate deviated wells.

## 1. INTRODUCTION AND MOTIVATIONS.

Sucker rod pumping is by far the most widely used means of artificial lift. In the past years, the wave equation has been used to compute downhole data using surface position and load as recorded by a dynamometer system. Most of the methods presently used are vertical-hole methods, i.e. they do not take into consideration the deviation of the well. For vertical wells, the only relevant friction forces are of viscous nature. However, when dealing with a deviated well, mechanical friction arises from the contact between the tubing, the rods and the rod couplings. Even though those forces can be ignored when the well is mostly vertical, they have to be accounted for when the well is deviated. If the algorithm used to compute the downhole data does not take into consideration the mechanical friction, the resulting downhole card can appear to be distorted. This condition cannot be helped by changing the viscous damping factors.

There exist numerous algorithms for the vertical-hole method. Snyder solved the wave equation using the method of characteristics, see [11], while Gibbs employed separation of variables and Fourier series; see [3, 4, 6]. In 1969, Knapp, see [7], introduced finite differences to solve the wave equation, which is also the method used by Everitt and Jennings in 1976, see [2, 9]. The Everitt-Jennings method has been implemented and modified by Weatherford International, see [1].

For the treatment of deviated wells, several methods are in existence to treat the Coulombs friction resulting from the mechanical friction, the best known of which was done by Gibbs, see [5] and by Lukasiewicz, see [8]. Gibbs modified the wave equation by adding a Coulombs friction term. Lukasiewicz derived equations for the axial and transverse displacement of the rod element, creating a system of coupled differential equations, which is also the approach taken in this paper.

In this paper, a finite difference approach is used to treat a system of two coupled non linear differential equations, which encompass the forces acting on a rod element in a deviated well. The axial displacement is taken into consideration as well as the transverse displacement of the rod element, providing a complete model for analyzing the downhole conditions. This paper utilizes equations as derived by Lukasiewicz in [8].

In Section 2, the equations for the axial and transverse displacement of the rod element are presented. In Section 3, the algorithm used for the solving of the system of coupled differential equations is presented. Finally in Section 4 conclusions are given.

This paper should be considered as a general algorithm outline. Further results and validation as well as details on the implementation will be available in future papers.

## 2. TANGENTIAL AND AXIAL FORCES.

The dynamic behavior of the rod string is different for deviated wells than for vertical wells. Indeed in vertical wells, the rod string is assumed to not move laterally. Also, the only friction to consider is the friction of viscous nature, since mechanical friction is not consequential enough to be considered. In deviated wells however, mechanical friction becomes non-negligible since there is extensive contact between the rods, the rod couplings and the tubing.

Also, since the well is deviated, some sections of the rod string can be bent between two couplings in the middle of a “dog leg” turn, which introduces the concept of curvature of the rod string.

Therefore in deviated wells, in addition to moving up and down, the rod string also moves laterally. While analyzing the behavior of the rod string, it is therefore essential to capture the behavior of the longitudinal stress waves as well as the lateral stress waves of the rod element.

In this section, the forces in the equation of motion in the axial and transverse directions are presented.

Let  $u(s, t)$  be the axial displacement of the rod element of length  $ds$ , and  $v(s, t)$  be the transverse displacement of the rod element. The radius of curvature  $R_\phi$  can be calculated along with the Cartesian coordinates of the wellbore path using the deviation survey. Several methods are available for such calculations such as the minimum curvature method or the radius-of-curvature method, see [5].

A diagram of the forces acting on the rod element is displayed in Figure 1. In Figure 1, the radius of curvature  $R_\phi$  is displayed as an arrow going from the center of the curvature to the rod element of length  $ds$ . The axial force denoted  $F$  is shown to act upwards and downwards on the rod element. The axial force, therefore, has an axial component as well as a transverse component. The Coulombs friction force labeled  $F_t$  opposes the movement of the rods at the point of contact between the rods and the tubing. The weight  $W$  is shown as a force pulling downward on the rod element. The normal force  $N$  is shown as a force acting perpendicularly on the rod element facing the center of curvature. Both the weight and the normal force have axial and transverse components.

In the tangential direction, using Newton’s second law we get:

$$\frac{\partial F}{\partial s} - A\gamma \frac{\partial^2 u}{\partial t^2} + \gamma g A \cos \theta - D \frac{\partial u}{\partial t} - F_t = 0, \quad (1)$$

Where  $A$  is the cross sectional area,  $\gamma$  is the density,  $g$  is the acceleration of gravity,  $\theta$  is the angle of inclination,  $D$  is the viscous damping coefficient,  $F_t$  is the friction force from the tubing,  $ds$  is the measured length of the rod,  $t$  is time.

The force  $F_t$  is the Coulombs friction force. Coulombs friction is a nonlinear force that tends to oppose the motion of bodies within a mechanical system. Coulombs friction is representative of dry friction, which resists relative lateral motion of two solid surfaces in contact. The relative motion of the rods, tubing and couplings pressing against each other is a source of energy dissipation when the well is pumping.

In the transverse direction, the equation of motion gives:

$$EI \frac{\partial^2}{\partial s^2} \left[ \frac{\partial^2 v}{\partial s^2} + \frac{1}{R_\phi} \right] + \gamma A \frac{\partial^2 v}{\partial t^2} + n_t + n_p + D_t \frac{\partial v}{\partial t} + \frac{F}{R} - \gamma g A \sin \theta = 0, \quad (2)$$

$$EI \frac{\partial^4 v}{\partial s^4} + EI \frac{\partial^2}{\partial s^2} \frac{1}{R_\phi} + \gamma A \frac{\partial^2 v}{\partial t^2} + n_t + n_p + D_t \frac{\partial v}{\partial t} + \frac{F}{R} - \gamma g A \sin \theta = 0.$$

Where  $EI$  is the bending stiffness,  $E$  is Young’s modulus of elasticity,  $I$  is the bending moment,  $D_t$  is the viscous damping factor in the lateral direction,  $n_t$  is the transverse normal force from the tubing,  $n_p$  is the transverse normal force from the liquid under pressure  $p$ .

As demonstrated by Lukasiewicz, the axial force can be introduced to (1) to give:

$$\frac{\partial^2 u}{\partial s^2} + \frac{\partial v}{\partial s} \cdot \frac{\partial^2 v}{\partial s^2} - \frac{1}{a^2} \frac{\partial^2 u}{\partial t^2} - \frac{D}{AE} \frac{\partial u}{\partial t} + \frac{\gamma g}{E} \cos \theta - \frac{F_t}{AE} = 0, \quad (3)$$

Where  $a$  is the acoustic velocity of the rod.

Furthermore, by assuming that the rod lies on the tubing in between couplings, equation (1) can be written as:

$$\frac{\partial^2 u}{\partial s^2} - \frac{1}{a^2} \frac{\partial^2 u}{\partial t^2} - \frac{D}{AE} \frac{\partial u}{\partial t} + \frac{\mu}{R} \frac{\partial u}{\partial s} + \frac{\gamma g}{E} \cos \theta - \frac{\mu}{E} (\gamma g \sin \theta) = 0, \quad (4)$$

For more details on the above equations and the axial force, see [8].

Equation (3) uses the surface position to calculate the downhole position at each finite difference node down the wellbore until the node right above the pump is reached.

Equations (3) and (2) are combined to form a system of two coupled nonlinear differential equation of fourth order. It is important to note that Coulombs friction, i.e. mechanical friction that arises from the contact between the rods, tubing, and rod couplings can be consequential in a deviated well and cannot be simulated using viscous damping. The Coulombs friction forces are not proportional to the velocity of the rod element as the viscous friction forces are. In some cases, the viscous damping factor can be increased to remove extra friction, but the downhole friction due to mechanical forces cannot be removed. If viscous damping is increased too much, the effects of the

mechanical friction can look like they have been removed, but in reality the downhole data no longer represents what is happening at the pump.

In equation (2), the second term is nonlinear and represents the effect of the vertical deflection on the axial displacement. Note that the equations given above are the same equations presented by Lukasiewicz in [8]. The model developed by Gibbs in [5] ignores the transverse movement of the rod string.

In the next section, the finite difference discretization is outlined and the algorithm presented.

### 3. FINITE DIFFERENCE DISCRETIZATION.

In this section, details on the finite difference discretization are given.

In the following, please note the subscript  $i$  represents the axial distance, while  $j$  represents time.

For the derivatives that appear in the above equations, Taylor series approximations are used to generate finite difference analogs. For the first and second derivatives, a first-order-correct central difference and second-order-correct central difference are used respectively. For more details on the derivation of the second derivative analog with respect to displacement, see [2].

For the space discretization, the finite difference analogs are:

$$\frac{\partial u}{\partial s_{i,j}} = \frac{(u_{i+1,j} - u_{i,j})}{\Delta s} - \frac{\Delta s}{2} \frac{\partial^2 u}{\partial s^2}, \quad \frac{\partial v}{\partial s_{i,j}} = \frac{(v_{i+1,j} - v_{i,j})}{\Delta s} - \frac{\Delta s}{2} \frac{\partial^2 v}{\partial s^2},$$

$$\frac{\partial^2 u}{\partial s^2_{i,j}} = \frac{(u_{i+1,j} - 2u_{i,j} + u_{i-1,j})}{\Delta s^2} - \frac{\Delta s^2}{12} \frac{\partial^4 u}{\partial s^4}, \quad \frac{\partial^2 v}{\partial s^2_{i,j}} = \frac{(v_{i+1,j} - 2v_{i,j} + v_{i-1,j})}{\Delta s^2} - \frac{\Delta s^2}{12} \frac{\partial^4 v}{\partial s^4}.$$

For the discretization in time, the finite difference analogs are:

$$\frac{\partial u}{\partial t_{i,j}} = \frac{(u_{i,j+1} - u_{i,j})}{\Delta t} - \frac{\Delta t}{2} \frac{\partial^2 u}{\partial t^2}, \quad \frac{\partial v}{\partial t_{i,j}} = \frac{(v_{i,j+1} - v_{i,j})}{\Delta t} - \frac{\Delta t}{2} \frac{\partial^2 v}{\partial t^2},$$

$$\frac{\partial^2 u}{\partial t^2_{i,j}} = \frac{(u_{i,j+1} - 2u_{i,j} + u_{i,j-1})}{\Delta t^2} - \frac{\Delta t^2}{12} \frac{\partial^4 u}{\partial t^4}, \quad \frac{\partial^2 v}{\partial t^2_{i,j}} = \frac{(v_{i,j+1} - 2v_{i,j} + v_{i,j-1})}{\Delta t^2} - \frac{\Delta t^2}{12} \frac{\partial^4 v}{\partial t^4}.$$

The analogs for the derivatives with respect to time are very straight forward. However, for the derivatives with respect to space of degree greater than one, the finite difference analogs must be split into several equations to accommodate different rod taper properties. The option to split the finite difference analogs into several equations primarily allows the user to pick  $\Delta s$  so that values for position, load and stress can be calculated at chosen steps down the wellbore as opposed to having to interpolate between fixed points. This option allows the user a greater freedom to refine the discretization to optimize stress analysis.

To handle the fourth order derivative with respect to displacement, a central finite difference scheme of second order is used:

$$\frac{\partial^4 v}{\partial s^4_{i,j}} = \frac{v_{i+2,j} - 4v_{i+1,j} + 6v_{i,j} - 4v_{i-1,j} + v_{i-2,j}}{\Delta s^4} - \frac{\Delta s^2}{6} \frac{\partial^6 v}{\partial s^6}.$$

In order to run a diagnostic model, equations (2) and (3) must be solved simultaneously.

Without loss of generality, as an initialization step, the rods can be assumed to lie on the tubing in order to solve for an initial  $u$ , i.e. we can assume  $v = 0$ .

In that case equation (4) can be solved first. Introducing the finite difference analogs into (4) yields:

$$u_{i+1,j} = u_{i,j} \left( \frac{\frac{\mu \Delta t^2 \Delta s}{R} + 2\Delta t^2 + 2\frac{\Delta s^2}{a^2} - \frac{D\Delta s^2 \Delta t}{AE}}{\Delta t^2 + \frac{\mu \Delta t^2 \Delta s^2}{R}} \right) + u_{i,j+1} \left( \frac{\frac{\Delta s^2}{a^2} - \frac{D\Delta s^2 \Delta t}{AE}}{\Delta t^2 + \frac{\mu \Delta t^2 \Delta s^2}{R}} \right) + u_{i-1,j} \left( \frac{-\Delta t^2}{\Delta t^2 + \frac{\mu \Delta t^2 \Delta s^2}{R}} \right) +$$

$$u_{i,j-1} \left( \frac{\frac{\Delta s^2}{a^2}}{\Delta t^2 + \frac{\mu \Delta t^2 \Delta s^2}{R}} \right) - \cos \theta \left( \frac{-\frac{\mu g \Delta s^2 \Delta t^2}{E}}{\Delta t^2 + \frac{\mu \Delta t^2 \Delta s^2}{R}} \right) + \gamma g \sin \theta \left( \frac{\frac{\mu \Delta s^2 \Delta t^2}{E}}{\Delta t^2 + \frac{\mu \Delta t^2 \Delta s^2}{R}} \right).$$

Next, still assuming  $\gamma = 0$ , equation (2) can be solved accordingly. Introducing the finite difference analogs into the axial force and equation (2) yields:

$$F = AE \left[ \frac{\partial u}{\partial s} \right] = AE \left( \frac{u_{i+1,j} - u_{i,j}}{\Delta s} \right),$$

$$v_{i+2,j} = 4v_{i+1,j} - 4v_{i-1,j} - v_{i-2,j} - v_{i,j} \left( 6 - \frac{2\gamma A}{\Delta t^2} - \frac{D_t}{\Delta t} \right) - v_{i,j+1} \left( \frac{\gamma A}{\Delta t^2} + \frac{D_t}{\Delta t} \right) - v_{i,j-1} \left( \frac{\gamma A \Delta s^4}{\Delta t^2 EI} \right) - u_{i+1,j} \left( \frac{A \Delta s^3}{RI} \right) - u_{i,j} \left( -\frac{A \Delta s^3}{RI} \right) - \left( \frac{\Delta s^4}{EI} \right) \left( NT + \frac{\pi p r^2}{R_\phi} - \gamma g A \sin \theta \right).$$

At this point initial values for  $v$  and  $u$  are available. Next equation (3) is solved. Introducing finite difference analogs into the axial force, the friction force and (3) reads:

$$F = AE \left[ \frac{\partial u}{\partial s} + \frac{1}{2} \left( \frac{\partial v}{\partial s} \right)^2 \right],$$

$$F = AE \left[ \frac{u_{i+1,j} - u_{i,j}}{\Delta s} + \frac{v_{i+1,j}^2 - 2v_{i+1,j}v_{i,j} + v_{i,j}^2}{2\Delta s^2} \right].$$

$$F_t = \frac{S}{R} \mu \Delta s,$$

$$F_t = \frac{AE\mu}{2R\Delta s} [2\Delta s(u_{i+1,j} - u_{i,j}) + v_{i+1,j}^2 - 2v_{i+1,j}v_{i,j} + v_{i,j}^2].$$

$$u_{i+1,j} = \frac{1}{\Delta s^2 - \frac{\mu}{R}} \left[ u_{i,j} \left( \frac{2}{\Delta s^2} + \frac{2}{\Delta t^2 a^2} - \frac{D}{AE\Delta t^2} - \frac{\mu}{R} \right) + u_{i-1,j} \left( -\frac{1}{\Delta s^2} \right) + u_{i,j+1} \left( \frac{1}{\Delta t^2 a^2} + \frac{D}{AE\Delta t^2} \right) + u_{i,j-1} \left( \frac{1}{\Delta t^2 a^2} \right) + v_{i+1,j}^2 \left( \frac{\mu}{2R\Delta s} - \frac{1}{\Delta s^3} \right) + v_{i,j}^2 \left( \frac{\mu}{2R\Delta s} - \frac{2}{\Delta s^3} \right) + v_{i+1,j} \cdot v_{i,j} \left( \frac{3}{\Delta s^3} - \frac{1}{\mu R \Delta s} \right) + v_{i-1,j} \cdot v_{i+1,j} \left( -\frac{1}{\Delta s^3} \right) + v_{i-1,j} \cdot v_{i,j} \left( \frac{1}{\Delta s^3} \right) - \frac{\gamma g}{E} \cos \theta \right].$$

Solving for  $u_{i+1,j}$  in the above system yields the downhole position. Load at the pump can then be computed using Hooke's law.

Please note that in practice, the second derivative and fourth derivative finite difference analogs with respect to space are split into several equations to adapt to different taper properties in a tapered string. A flowchart of the algorithm is given in Figure 2.

Also incorporated in the above algorithm is a single or dual iteration on the damping factor. Since the numerical methodology for solving the system of coupled nonlinear differential equation is similar to the numerical implementation of the modified Everitt-Jennings method, a similar iterative method can be used to calculate the net stroke and damping factor. For more details, see [9].

#### 4. CONCLUSIONS.

The ability to include the mechanical friction when dealing with deviated wells has been a growing concern in the industry. Often, users try to remove downhole friction from a downhole card by modifying the viscous damping factor, which essential falsifies the downhole results and hides existing downhole conditions. Since the overall methodology is similar to the modified Everitt-Jennings numerical solution, single or dual iteration on the damping factor can still be used to optimize the resolution of viscous damping. Using finite differences to solve the system of coupled differential equations is a convenient method for analyzing stress in a sucker-rod system. By splitting the finite difference analogs for the space discretization, this allows the above equations to be valid for tapered rod strings, including steel rods and fiberglass rods with sinker bars. Including Coulombs friction in downhole analysis, in the case of a deviated well, gives a better approximation of the downhole conditions than using a vertical-hole model.

The algorithm presented in this paper, when applied as a diagnostic tool, generates the true downhole card, without the excess downhole friction caused by deviation and with optimal viscous damping. This algorithm is essential when controlling wells using downhole data.

#### ACKNOWLEDGEMENTS

Special thanks to Dr. S. Lukasiewicz and the team here at Weatherford.

#### BIBLIOGRAPHY.

1. Ehimeakhe, V. : "Comparative Study of Downhole Cards Using Modified Everitt-Jennings Method and Gibbs Method", Southwestern Petroleum Short Course 2010.
2. Everitt, T. A. and Jennings, J. W.: "An Improved Finite-Difference Calculation of Downhole Dynamometer Cards for Sucker-Rod Pumps," paper SPE 18189 presented at the 63<sup>rd</sup> Annual Technical Conference and Exhibition, 1988.
3. Gibbs, S. G., and Neely, A. B. : "Computer Diagnosis of Down-Hole Conditions in Sucker Rod Pumping Wells," JPT (Jan. 1996) 91-98; *Trans.*, AIME,237
4. Gibbs, S. G.: "A Review of Methods for Design and Analysis of Rod Pumping Installations," SPE 9980 presented at the 1982 SPE International Petroleum Exhibition and Technical Symposium, Beijing, March 18-26.
5. Gibbs, S. G.: "Design and Diagnosis of Deviated Rod-Pumped Wells", SPE Annual Technical Conference and Exhibition, Oct 6-9, 1991, Dallas, USA.
6. Gibbs, S.G.: "Method of Determining Sucker-Rod Pump Performance," U.S. Patent No. 3,343,409 (Sept. 26, 1967).
7. Knapp, R. M.: "A Dynamic Investigation of Sucker-Rod Pumping," MS thesis, U. of Kansas, Topeka (Jan. 1969).
8. Lukasiewicz, S. A.: "Dynamic Behavior of the Sucker Rod String in the Inclined Well", Production Operations Symposium, April 7-9, 1991, Oklahoma City, Oklahoma, USA.
9. Pons-Ehimeakhe, V.: "Modified Everitt-Jennings Algorithm With Dual Iteration on the Damping Factors," 2012 SouthWestern Petroleum Short Course, Lubbock, Texas, April 18-19.
10. Schafer, D. J. and Jennings, J. W.: "An Investigation of Analytical and Numerical Sucker-Rod Pumping Mathematical Models," paper SPE 16919 presented at the 1987 SPE Annual Technical Conference and Exhibition, Dallas, Sept. 27-30.
11. Snyder, W. E.: "A Method for Computing Down-Hole Forces and Displacements in Oil Wells Pumped With Sucker Rods," paper 851-37-K presented at the 1963 Spring Meeting of the API Mid-Continent District Div. of Production, Amarillo, March 27-29.

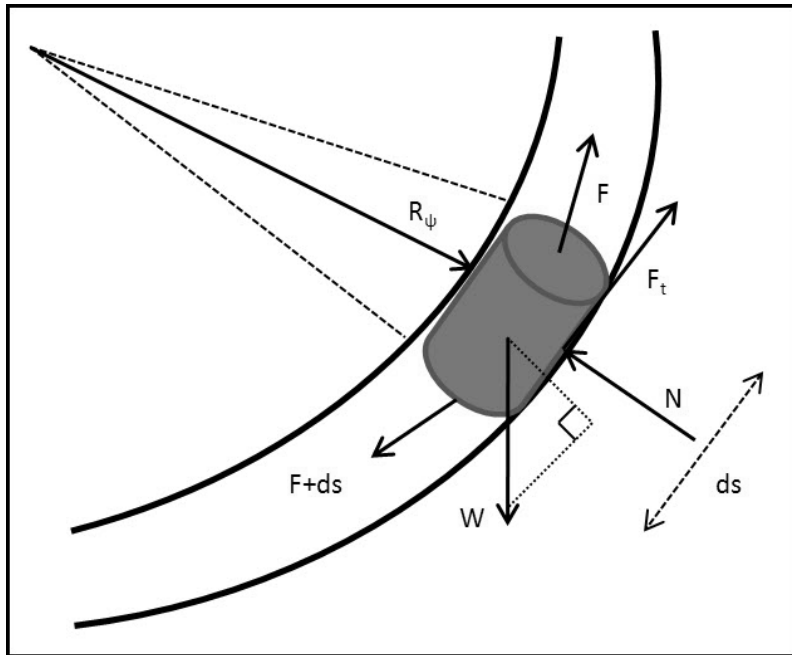


Figure 1 - Diagram of the forces applying to the rod element in a deviated well.

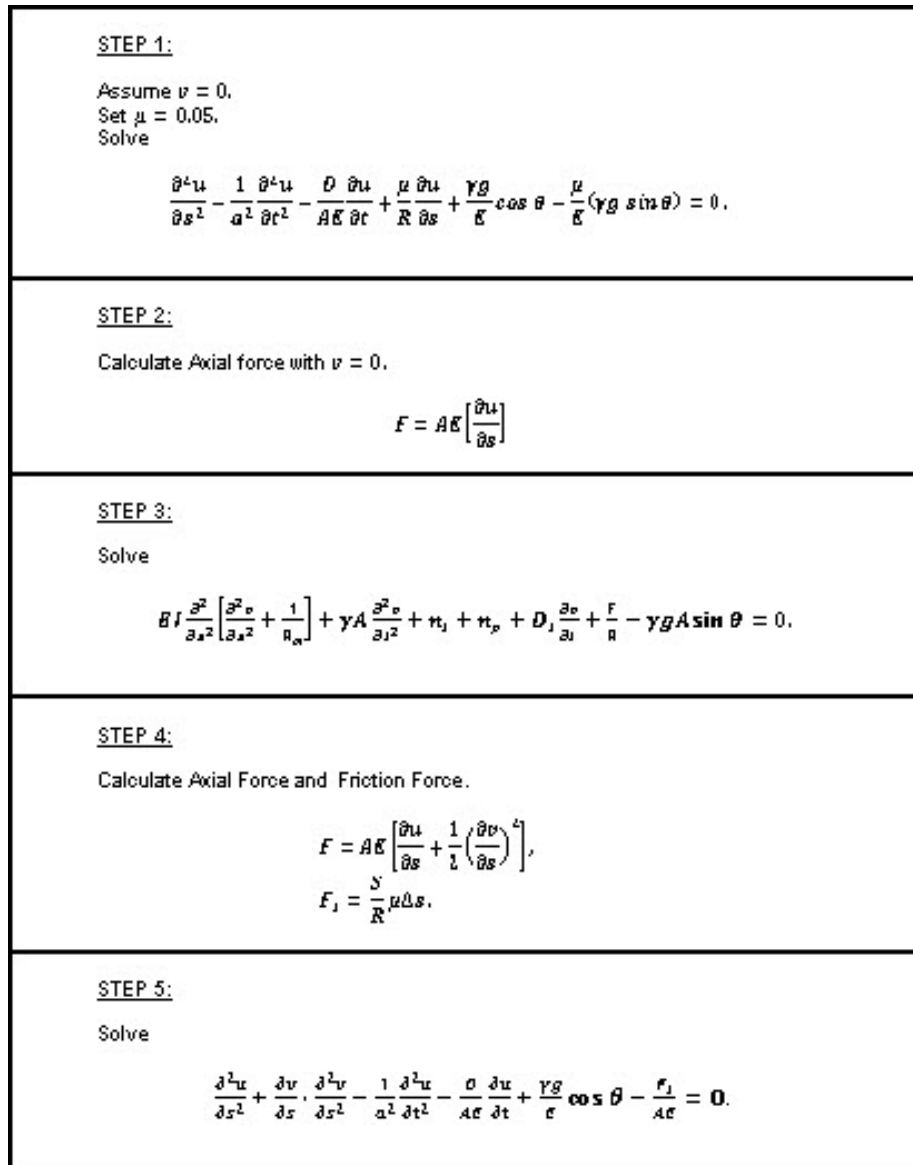


Figure 2 - Flowchart of the Diagnostic Algorithm